

Enhancing Gas Transmission Rate of PBS/PBAT Composite Films: A Study on Microperforated Film Solutions for Mango Storage

Charinee Winotapun,* Methinee Tameesrisuk, Pakjira Sirirutbunkajal, Pichamon Sungdech, and Pattarin Leelaphiwat



Cite This: *ACS Omega* 2024, 9, 3469–3479



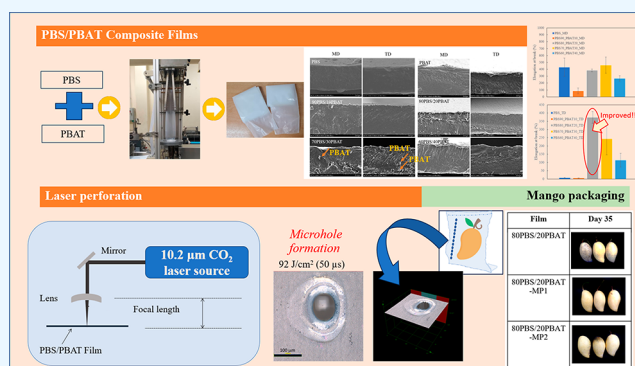
Read Online

ACCESS |

Metrics & More

Article Recommendations

ABSTRACT: This study focused on improving the mechanical properties of the poly(butylene succinate) (PBS) film by incorporation of poly(butyrate adipate terephthalate) (PBAT). At 20 wt % PBAT, elongation in the transverse direction improved by 373% while maintaining high tensile strength (27 MPa) and Young's modulus (262 MPa). The PBS80/PBAT20 composite film exhibited optimized mechanical properties. The absorbance coefficient of microperforated film at 980/cm for the 80PBS/20PBAT mix, corresponding to the 10.2 μm CO₂ laser wavelength, was 65/cm, indicating high film capability to absorb energy from the CO₂ laser. The introduction of microholes enhanced the gas permeability of the PBS/PBAT film. As fluences increased from 187 to 370 J/cm², there was a notable increase in microhole area in 80PBS/20PBAT film from 19,375 to 46,421 μm^2 . Concurrently, the gas transmission rate for a singular hole increased from 45 to 210 cm³/d for the oxygen transmission rate (OTR) and from 115 to 220 cm³/d for the CO₂ transmission rate (CO₂TR). For mango packed in microperforated 80PBS/20PBAT films, the O₂ levels inside the package gradually dropped and remained at 14.2% in PBS80/PBAT20-MP1 (OTR \sim 68,900 cm³/m²·d) and 16.7% in PBS80/PBAT20-MP2 (OTR \sim 131,900 cm³/m²·d), while CO₂ content increased to 6% for PBS80/PBAT20-MP1 and 4% for PBS80/PBAT20-MP2 throughout 33 days. On day 2 of storage in the nonperforated package, O₂ content dropped to 2% while CO₂ content rose to 22%. Mango packed in the 80PBS/20PBAT film package exhibited an unsatisfactory freshness quality due to the detection of a fermentative odor on day 5 of the storage period. Total soluble solids, color, and weight loss of mango remained stable during storage in all microperforated films. Results demonstrated that the mango shelf life was significantly extended by 35 days using 80PBS/20PBAT-MP1. Laser perforation offered a practical method for improving gas transmission rates (OTR and CO₂TR) of 80PBS/20PBAT film for mango packaging.



1. INTRODUCTION

Modified atmosphere packaging (MAP) is a novel technology that can control gas composition inside the package to maintain freshness and extend the shelf life of fruits and vegetables.^{1–4} Highly respiring produce requires modification of the O₂ and CO₂ levels in packaging. Gas composition changes within the packaging film depend on various factors such as the weight of the produce, respiration rate, package size, and gas permeability of the film.^{5–8} By controlling the gas composition, MAP effectively reduces the respiration rate and dehydration of fresh fruits and vegetables, thus retarding deterioration and extending the shelf life.^{9–11} Plastic films with an oxygen transmission rate (OTR) of over 10,000 cm³/m²·d can induce a desirable modified atmosphere within fresh produce packaging throughout the storage period.¹²

Environmental concerns regarding plastic food packaging waste have recently increased, with both packaging manufacturers and consumers becoming more conscious of the use of

petroleum-based plastic films.^{4,13,14} The development of biodegradable films made from natural resources offers a solution to the critical problem of plastic waste disposal, replacing fossil-oil-based packaging materials. Biodegradable polymer packaging, such as poly(butylene succinate) (PBS) and poly(butyrate adipate terephthalate) (PBAT), has gained traction due to favorable processability and excellent mechanical and biodegradable properties.^{15–17} These materials are appropriate for packaging applications, but one drawback associated with biodegradable polymer packaging is the inherently low gas permeability, limiting its suitability for

Received: September 13, 2023

Revised: November 23, 2023

Accepted: December 14, 2023

Published: January 9, 2024



preserving the freshness of perishable commodities.^{18,19} Gas permeability of biodegradable plastic films can be improved by using laser perforation technology.^{20,21} When a laser beam is directed onto the film surface, energy is absorbed, generating heat that melts and removes the plastic material, resulting in the formation of small holes. Microperforated films are now used in the packaging of fresh food products using MAP.^{2,4,3,22,23} This cost-effective technique enhances the gas transport properties of the packaging films by introducing microperforations as tiny holes with diameter of less than 300 μm .²⁴ Successful perforation of microholes is dependent on several factors, such as material properties and the laser perforation process. Material properties include the type of material, thickness, thermal conductivity, heat capacity, and additives, while laser wavelength, fluence, and pulse duration are perforation process parameters.²⁵ Oxygen and carbon dioxide transmission rates (OTR and CO_2TR) of laser microperforated films can be controlled by varying the size and number of holes.

Mangifera indica cv. "Nam Dok Mai Si Thong" is a popular variety of mango in Thailand famous for its distinct flavor, aroma, and bright yellow color. "Nam Dok Mai Si Thong" means golden sweet fragrance, emphasizing its appealing qualities. Compared to other fruits, mangoes have a high respiration rate.²⁶ During the respiration process, mangoes consume oxygen and release carbon dioxide, along with other metabolic byproducts. Temperature, maturity stage, and variety are the main factors contributing to the high respiration rate. High temperatures generally increase the respiration rate of mangoes, leading to faster ripening and shorter shelf life, while respiration rate is also significantly influenced by the fruit maturity stage.²⁷ Mangoes ripen quickly at ambient temperature, with the respiration rate increasing as they progress from unripe to ripe stage. To maximize shelf life, the maturity of mangoes must be controlled by keeping the fruit at an appropriate temperature to decrease respiration and maintain quality. Storing mangoes at low temperatures, typically 10–13 °C, decreases their respiration rate and extends their shelf life.²⁸ However, extremely low temperatures can result in chilling injury causing internal breakdown, surface pitting, discoloration, and decay.²⁹ Consequently, it is important to maintain an appropriate balance. To manage the high respiration rate of mangoes and prolong their shelf life, proper postharvest handling and storage practices such as temperature-controlled atmosphere storage must be followed. Controlled atmosphere storage or modified atmosphere storage techniques such as MAP can regulate the gas composition surrounding the fruit, retard respiration, and delay ripening. Boonruang et al.³⁰ examined the effects of utilizing various packaging films (nonperforated highly gas-permeable film, nonperforated ethylene-absorbing highly gas-permeable film, microperforated highly gas-permeable film, and nonperforated polyethylene film) to maintain quality and extend shelf life of "Nam Dok Mai" mango. Their results suggested that ethylene-absorbing films prolonged the mango shelf life to 40 days. An equilibrium-modified atmosphere had a significant impact on the quality and shelf life of fresh mangoes and was closely related to the gas permeability of the films. Phakdee and Chairasart³¹ studied shelf life extension of mangoes packed in MAP using ethylene-absorbing bags. The mangoes were stored at 15 °C for 30 days. The MAP technique effectively retarded the ripening process and delayed color development, contrasting with fruits that were not

packed and stored under the same cold storage conditions. The ethylene absorbing bag significantly reduced the respiration rate and weight loss of the fruits throughout the 30-day storage period at 15 °C. Srinivasa et al.³² investigated the effect of modified atmosphere packaging on the quality of mango fruits. The fruits were stored at room temperature in carton boxes, with the top surface covered with either chitosan film or low-density polyethylene. On day 3, CO_2 and O_2 levels were 23–26% and 3–6%, respectively, and at the end of the storage period, they were 19–21% and 5–6%, respectively. Fruits stored in chitosan-covered boxes, on the other hand, had a shelf life extension of up to 18 days with no microbial growth or off flavor. The films made from chitosan are useful as an alternative to synthetic packaging films in the storage of freshly harvested mangoes, because they are biodegradable and environmentally friendly. Several studies have proposed the use of modified atmosphere packaging (MAP) with ethylene-absorbing bags to extend the shelf life of mangoes. However, these ethylene-absorbing bags are costly. Therefore, there is growing interest in cost-effective techniques that improve the gas transport properties of packaging films by introducing microperforations to extend the shelf life of mangoes.

Copious researches^{2,22,33} have explored the application of polypropylene and poly(ethylene terephthalate)/polyethylene laminated films as microperforated solutions for modified atmosphere packaging (MAP) of fresh fruits and vegetables; however, detailed research into laser perforation of biodegradable films, especially PBS/PBAT, remains limited. This study investigated the process of creating microholes in PBS/PBAT biodegradable films via laser perforation. The essential parameters such as the film absorption coefficient and laser fluence that impact the perforation process were examined. The relationship between the number of microholes and resultant gas permeability was also explored to determine the efficacy of microperforated biodegradable films in prolonging mango freshness. Comprehensive analyses of the gas composition within the packaging, mango firmness, soluble content, color variations, and weight degradation during storage were also conducted.

2. MATERIALS AND METHODS

2.1. Materials. Commercial grade poly(butylene succinate) (PBS), known as FZ92PM, was sourced from PTT MCC Biochem Co., Ltd., Thailand with a density and melt flow index of 1.26 g/cm^3 and 5 $\text{g}/10$ min (190 °C, 2.16 kg), respectively. Jin Hui Zhao Long High Tech Co., Ltd. provided Ecoworld grade commercial PBAT with a density of 1.26 g/cm^3 and melt flow index of 3–5 $\text{g}/10$ min (190 °C, 2.16 kg).

2.2. Preparation of PBS/PBAT Blended Film. PBS/PBAT blended films of various compositions were produced by blown film extrusion (Haake PolyLab OS RheoDrive 7 model, Germany), using 29 mm screw diameter, 25 L/D ratio, and 3:1 compression ratio with a 35 mm-diameter annular die and 1 mm die gap. The polymers were extruded at 60 rpm screw speed with the die set to 160 °C and barrel temperatures maintained at 150, 155, and 160 °C. The produced films were 40 μm thick with a 4 kg/h output rate. The blown film extrusion process had a blowup ratio (BUR) of 2.5, a takeup ratio (TUR) of 4.9, and a forming ratio (FR) of 1.9.

2.2.1. PBS/PBAT Blended Film Characterization.
2.2.1.1. Film Mechanical Testing. The mechanical characteristics of at least five samples of each film were examined using a universal testing device (model 5943, Instron, USA), with a

load cell of 100 N, crosshead speed of 500 mm/min, and 50 mm gauge length. Tensile strength, Young's modulus, and elongation at break were investigated using ASTM standard D882-02.

2.2.1.2. Scanning Electron Microscopy (SEM). To determine the microstructure of the blends, images of the cross-sectional view of the films were analyzed using a scanning electron microscope (SEM) (SU5000, Hitachi, Japan) operating at an accelerating voltage of 5 kV. To avoid charging and to lessen the possibility of phase deformation, the samples were cryogenically fractured in liquid nitrogen and coated with gold. Cross-sectional morphology was investigated in both the machine and transverse directions (MD and TD).

2.2.1.3. Fourier-Transform Infrared Spectroscopy (FTIR). The absorption coefficients of the blended films were calculated by measuring the FTIR absorption spectra. A Fourier-transform Infrared Spectrometer (Shimadzu, IR-Tracer-100, Japan) with a frequency range of 4000 to 400/cm was used to obtain the FTIR spectra of the films. The 10.2 μm wavelength of the CO₂ laser corresponded to a frequency band at 980/cm. The absorption coefficient α (/cm) was calculated using eq 1

$$\alpha = -\frac{1}{z} \ln \frac{I}{I_0} \quad (1)$$

where z is the film thickness, and I and I_0 are the transmitted light intensity and the incident light intensity, respectively. The thickness of the film was approximately 40 μm . A minimum of three samples were tested, and results were reported as averages and standard deviations.

2.3. Laser Perforation Process. Perforation of the PBS/PBAT blended film was carried out by using a CO₂ laser (Synrad, Ti60 model, USA) with a wavelength of 10.2 μm and a power output of 50 W. The laser setup included a focusing lens with a focal length of 25.4 mm and a focal spot diameter of 83 μm , as shown in Figure 1. The biodegradable films were

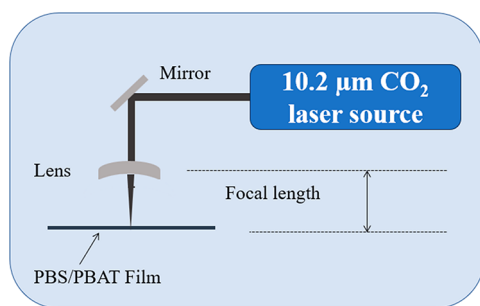


Figure 1. Schematic of the laser perforation process.

exposed to the laser beam while moving at a speed of 10 m/min. To achieve the desired results, different laser fluences ranging from 37 to 370 J/cm², corresponding to pulse durations of 20 to 200 μs , were used to irradiate the plastic film at the focal point.

2.3.1. Microperforated PBS/PBAT Blended Film Characterization. **2.3.1.1. 3D Laser Scanning Confocal Microscope.** A three-dimensional (3D) laser scanning confocal microscope (LEXT OLS4100, Olympus, Japan) was used to examine the surface morphologies of the microholes on the film surface. Microhole dimensions were measured in both the machine direction (MD) and transverse direction (TD) using a minimum of three samples.

2.3.1.2. Gas Transmission Rates. Gas transmission rates of the microperforated films were assessed using the static method under controlled conditions of 25 °C and 60% relative humidity (RH), following the protocol summarized by Winotapun et al.³⁴ A cylindrical acrylic container 1610 cm³ was used, with microperforated film (test film area 103 cm²) as the top lid tightly clamped in place with an acrylic ring. Gas valves for the inlet and outlet were carefully regulated in the chamber. To eliminate residual gas, a gas mixture containing 21% CO₂, 0% O₂, and 79% N₂ was introduced into the chamber at a flow rate of 250 cm³/min for 6 h. After closing of the inlet and outlet valves, a gas sample of 6 cm³ was collected from the cylinder after 1 day and analyzed using a gas analyzer (Dansensor CheckPoint 3, Mocon, Denmark). Oxygen and carbon dioxide transmission rates through the microholes were calculated following the methodology explained by Winotapun et al.³⁴ The overall gas transmission rate was determined by considering both film and microhole transmission. The gas transmission rate through a perforated microhole was obtained by subtracting the gas transmission rate of the film without microholes from the total gas transmission rate. All measurements were performed in triplicate.

2.4. Plant Material and Packaging Films. Shine Forth Co., Ltd., Thailand provided mango (*Mangifera indica* L. cv. "Nam Dok Mai") fruits appropriate for export. Consistent maturity (80%) with a weight range of 350 \pm 50 g were selection criteria. The mangoes were washed in a 200 ppm of NaOCl solution and then dipped for 5 min in hot water at 52 \pm 2 °C. The fruits were air-dried naturally at room temperature. Each mango fruit was individually sealed in a plastic bag 15 cm \times 22 cm and stored at 13 °C. The total volume of the packaging was approximately 1250 cm³. The headspace volume was approximately 400 cm³.

2.4.1. Quality Assessment. **2.4.1.1. Atmosphere Composition Inside Packages.** The O₂ and CO₂ compositions inside the packaging were analyzed in triplicate by using a CheckMate Headspace Gas Analyzer from Dansensor A/S, Denmark. The volume of the gas composition measured was 6 cm³.

2.4.1.2. Firmness. Firmness was measured using a penetrometer (Fruit Firmness Tester FT-011, Palalyne Company Limited, UK) with a 5 mm diameter puncture probe to a penetration depth of 10 mm. Values were reported in Newton unit. A minimum of three samples were tested. The average values and standard deviations were reported.

2.4.1.3. Weight Loss Percentage. The mango was weighed before and after packing with a digital weighing balance (Mettler PB5001, Mettler Toledo AG, Canada). Weight loss percentage of mango was calculated using eq 2 by subtracting the weight during the storage period (W_t) from the initial weight (W_i). All measurements were taken at least in quintuplicate.

$$\% \text{Weight loss} = \frac{(W_i - W_t)}{W_i} \times 100 \quad (2)$$

2.4.1.4. Total Soluble Solids (TSS). TSS were quantified for each sample using a standard °Brix unit on an Atago digital refractometer (Atago Co. Ltd., Japan) at 25 °C. The measurements were repeated three times.

2.4.1.5. Color. The color change of mango pulp was assessed using a MiniScan EZ 4500L Spectrophotometer from HunterLab, USA. A minimum of five measurements were taken at the center of each mango. The L^* , a^* , and b^* values were

Table 1. Mechanical Properties of PBS/PBAT Compositd Films^a

Mechanical properties		PBS	90PBS/10PBAT	80PBS/20PBAT	70PBS/30PBAT	60PBS/40PBAT
Tensile strength at max load (MPa)	MD	46 ± 10	32 ± 1	37 ± 3	35 ± 8	38 ± 8
	TD	32 ± 3	22 ± 2	27 ± 4	20 ± 4	18 ± 8
Young's Modulus (MPa)	MD	351 ± 90	387 ± 54	318 ± 24	225 ± 39	217 ± 54
	TD	471 ± 64	262 ± 43	262 ± 75	207 ± 57	109 ± 38
Elongation at break (%)	MD	480 ± 20	100 ± 39	362 ± 59	424 ± 79	267 ± 38
	TD	7 ± 1	6 ± 0	373 ± 35	243 ± 97	132 ± 54

^aData are reported as mean ± standard deviation.

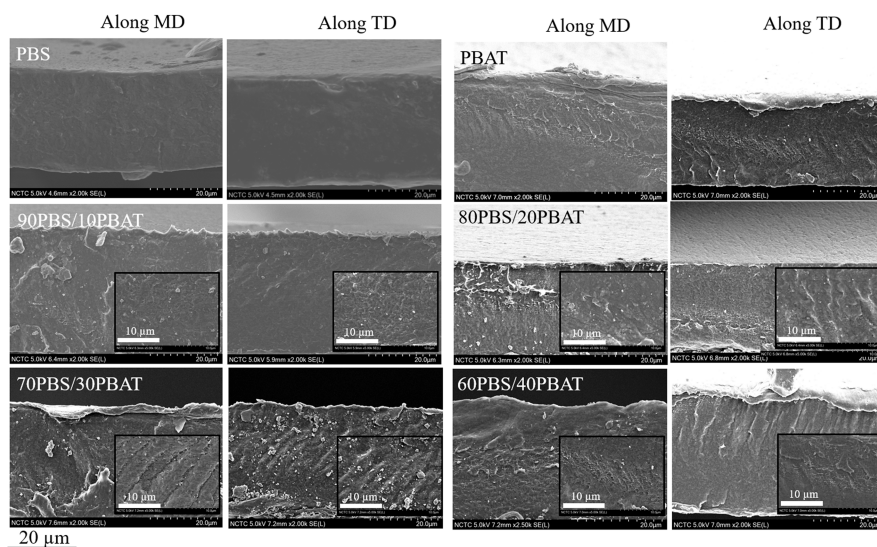


Figure 2. SEM micrographs of cross-sectional surface images of PBS, PBAT, 90PBS/10PBAT, 80PBS/20PBAT, 70PBS/30PBAT, and 60PBS/40PBAT films at magnifications of 1000× and 5000×.

analyzed. L^* represents the lightness of the samples, ranging from a maximum value of 100 (light) to a minimum of zero (dark). Positive a^* values indicate redness, while negative a^* values signify greenness. Similarly, positive b^* values correspond to yellow, and negative b^* values indicate blue. At least five measurements were taken in the center of each mango sample.

3. RESULTS AND DISCUSSION

3.1. Characterization of Biodegradable PBS/PBAT Film. **3.1.1. Mechanical and Morphological Properties of PBS/PBAT Film.** The mechanical properties of the composite polymer films, with an almost uniform thickness of 40 μm , were examined by following ASTM D882. Since variations in sample thickness can directly impact tensile strength measurements, it is necessary to control and maintain a uniform sample thickness. The PBS/PBAT blended films were tested at various compositions of PBAT ranging from 10 to 40 wt %. Experimental results of mechanical properties in the MD and TD are shown in Table 1. Tensile strength, Young's modulus, and elongation at break of neat PBS in the machine direction (MD) were 46 MPa, 351 MPa, and 480%, respectively, with results in the transverse direction (TD) 32 MPa, 471 MPa, and 7%. Due to the film-forming process, tensile strength and elongation at break of the film in the MD were greater than in the TD. The polymer chain in film winding was tensioned in the MD during blown film extrusion, resulting in molecular chain orientation aligning in the machine direction rather than in the transverse direction, directly affecting the mechanical properties of the film. However, with only 7% elongation at the

break in the TD, the neat PBS film was inadequate for packaging applications. To improve the elongation at break, PBAT was added to the PBS film. When 10 wt % PBAT was added to the PBS film, most of the mechanical properties in the MD and TD directions reduced, but elongation at break in the TD did not improve. The SEM images (Figure 2) showed that tensile properties were related to morphological observations. The cross-sectional surface images of neat PBS film were smoother than neat PBAT in both MD and TD. Addition of 10% PBAT to PBS resulted in the formation of dispersed phases characterized by small spherical structures. Increasing the proportion of the dispersed phase caused a decrease in the tensile strength. This phenomenon was attributed to phase separation, suggesting that a heterogeneous blend within the system resulted in weak interaction between the PBS and PBAT phases.³⁵ When the PBAT content increased to 20 wt %, elongation in the TD significantly increased by 373% while maintaining high tensile strength (27 MPa) and Young's modulus (262 MPa). PBAT exhibited a significantly higher elongation at break compared to that of PBS due to its higher flexibility. This result was consistent with results reported by Boonprasertpoh et al.³⁵ They stated the same phenomenon with PBS/PBAT blends, namely, that elongation at break of the blends increased as PBAT content increased. However, adding PBAT above 20 wt % led to instability during film blowing. When PBS was mixed with PBAT at a concentration of 30%, the PBAT phase agglomerated (implying an immiscible blend) and the mechanical properties of the film reduced.³⁶ Notably, no phase agglomerations were observed in the 60PBS/40PBAT

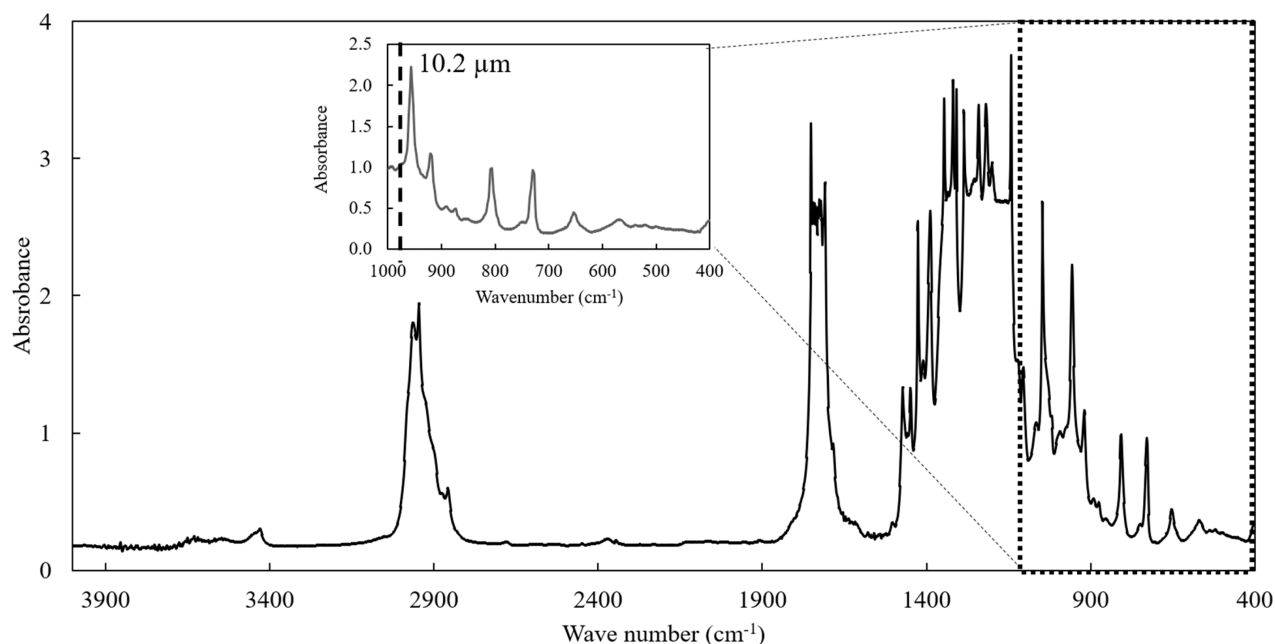


Figure 3. FTIR spectra of 80PBS/20PBAT film at wave numbers from 4000 to 400/cm.

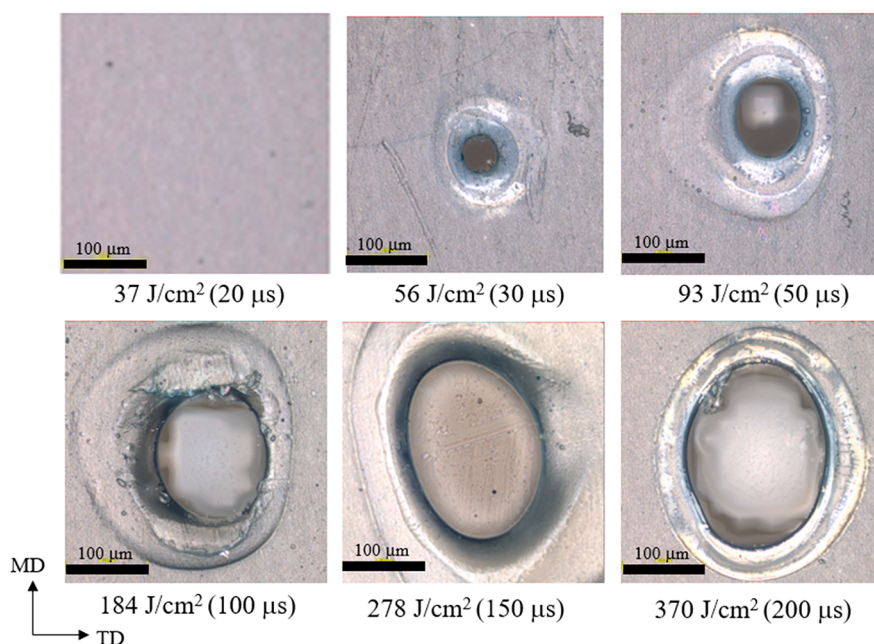


Figure 4. Laser scanning confocal images of single microholes on the 80PBS/20PBAT film surface at laser fluence 37 to 370 J/cm² corresponding to pulse duration of 20 to 200 μs.

blend because PBAT formed a cocontinuous phase, as can be seen in Figure 2. In a study by Boonprasertpoh et al.,³⁵ the rheological properties of PBS blended with 40 to 50 wt % PBAT were investigated using a rotational rheometer in frequency sweep mode. In the case of the PBS major phase blended with low PBAT content, it was observed that the PBS/PBAT blends exhibit higher complex viscosity than neat PBS due to the result of a dispersed phase having interactions or entanglements with the matrix phase. For PBS blended with 40 to 50 wt % PBAT, the complex viscosity at frequencies greater than 0.03 rad/s was lower compared to neat PBS, suggesting weak interaction between the PBS and PBAT phases. In

addition, bubble instability of 60PBS/40PBAT in blown film extrusion process occurred.³⁶

3.1.2. Fourier-Transform Infrared Spectroscopy (FTIR). A carbon dioxide (CO₂) laser with a wavelength of 10.2 μm long infrared was used as the photothermal mechanism. Laser energy was absorbed by the plastic film, generating heat and causing melting, resulting in hole creation. FTIR spectrometry was used to determine the absorption coefficient of the film. The 10.2 μm laser wavelength corresponded to a wavenumber of 980/cm. The PBS80/PBAT20 film which exhibited optimized mechanical properties was selected for analysis. Figure 3 shows the FTIR spectra of 80PBS/20PBAT film at wave numbers ranging from 4000 to 400/cm. Using eq 1, the

Table 2. Microhole Area, Diameter, and Aspect Ratio at Various Laser Fluences

Laser fluence (J/cm ²)	Pulse duration (μm)	Hole area (μm ²)	Diameter in MD (μm)	Diameter in TD (μm)	Aspect ratio (MD/TD)
56	30	1743 ± 383	50 ± 4	47 ± 5	1.05
92	50	7721 ± 673	98 ± 3	85 ± 2	1.15
184	100	19,375 ± 804	181 ± 9	134 ± 4	1.35
278	150	31,709 ± 4498	223 ± 4	175 ± 24	1.27
370	200	46,421 ± 3854	280 ± 15	210 ± 9	1.33

Table 3. Gas Transmission Rates of 80PBS/20PBAT Film with Various Numbers of Microholes at Laser Fluence 370 J/cm²

Number of microholes/ 103 cm ²	Pulse duration (μs)	Laser fluence (J/cm ²)	Gas transmission rate								
			Average through-microhole area and diameter			Microperforated film ^a			Microhole		
			MD	TD	Area μm ²	OTR/103 cm ² , (cm ³ /d)	CO ₂ TR/103 cm ² , (cm ³ /d)	CO ₂ TR/ OTR/ 103 cm ²	OTR/hole (cm ³ /d)	CO ₂ TR/hole (cm ³ /d)	O ₂ TR/ OTR
0						61 ± 0	170 ± 15	2.78			
1	100	184	181 ± 9	134 ± 4	19,375 ± 804	106 ± 13	284 ± 6	2.68	45 ± 13	115 ± 15	2.53
	150	278	223 ± 4	175 ± 24	31,709 ± 4,498	155 ± 8	305 ± 17	1.97	94 ± 8	135 ± 17	1.44
	200	370	280 ± 15	210 ± 9	46,421 ± 3,854	271 ± 7	390 ± 33	1.44	210 ± 7	220 ± 33	1.05
	200	370	280 ± 15	210 ± 9	46,421 ± 3,854	846 ± 125	785 ± 139	0.93	785 ± 125	615 ± 139	0.78
5	200	370	280 ± 15	210 ± 9	46,421 ± 3,854	1332 ± 199	1285 ± 127	0.96	1271 ± 199	1115 ± 127	0.88

^aTest film area of 103 cm². Data are reported as mean ± standard deviation.

absorbance coefficient at 980/cm of 80PBS/20PBAT was 65/cm, providing material-specific information. Results indicated the capability of the film to absorb energy from a 10.2 μm CO₂ laser.

3.2. Laser Perforation Process. **3.2.1. Surface Morphologies of Microholes on PBS/PLA Film Surfaces.** A CO₂ laser was used to irradiate the PBS/PBAT film surface, with laser fluences ranging from 37 to 370 J/cm², corresponding to laser pulses ranging from 20 to 200 μs. The PBS/PBAT film was irradiated at a constant web speed of 10 m/min. The morphologies of the 80PBS/20PBAT film in the laser focusing area are listed in Figure 4. When the laser fluence was less than 56 J/cm², the film was unaffected. At a fluence of 56 J/cm², the 80PBS/20PBAT film initially formed microholes. The fluence level represents the minimum amount of energy needed to perforate the PBS/PBAT film. The 80PBS/20PBAT film (with an absorption coefficient of 65/cm) exhibited a high absorption coefficient, leading to a significant increase in the temperature on the film surface. The opening of microholes occurred at a fluence of 56 J/cm². The perforation threshold indicates the lowest fluence at which microhole formation occurs on a plastic film.³⁴ The film was melted and removed within the laser focus area during laser processing, resulting in a concave depression surrounded by an elevated polymer rim. Increasing the laser fluence resulted in the formation of microholes. The 80PBS/20PBAT film first exhibited microholes at a fluence of 56 J/cm². The size of the microholes, in terms of area and diameter, increased as the laser fluence increased. As the laser energy was absorbed, the polymer melted due to the rise in surface temperature caused by thermal conduction. Hence, the microhole area and diameter expanded with increasing laser fluence.²⁵ Increasing the laser fluence on the 80PBS/20PBAT film from 56 to 370 J/cm² resulted in an increase in microhole area on the 80PBS/20PBAT surface from 1743 to 46,421 μm².

Each microhole began with an elliptical shape, as shown in Figure 4. The diameter of the microhole was greater in the machine direction (MD) than in the transverse direction (TD). Table 2 shows the corresponding values for the

microhole diameter measured in the MD and TD. Because of the fixed laser head and the film web speed of 10 mm/min, the aspect ratio (MD/TD) of the hole diameter exceeded 1. The elongated shape of the microhole at high laser fluences above 92 J/cm² was caused by continuous heating in the film moving direction caused by the heat-affected zone on the focused film surface.² The aspect ratio of the microhole increased from 1.15 to 1.33 as the laser fluence increased from 92 to 370 J/cm² or, equivalently, as the pulse duration increased from 50 to 200 μs.

3.2.2. Gas Transmission Rates. The gas transmission rate of the 80PBS/20PBAT film with a thickness of 40 μm was investigated. In a previous study,³⁷ it was noted that the gas transmission rate decreased with an increase in film thickness. Variations in the sample thickness can directly impact the diffusion of gases through the polymer matrix. Therefore, it is necessary to maintain a consistent sample thickness when comparing films. For gas transmission rates measurement, the 80PBS/20PBAT film without perforations showed oxygen transmission rate (OTR) and carbon dioxide transmission rate (CO₂TR) of 61 ± 0 cm³/d and 170 ± 15 cm³/d, respectively, for a test area of 103 cm². Nonperforated films had a CO₂TR to OTR ratio (β) of 2.78. Gas transmission rates improved significantly with microholes, as shown in Table 3. The gas transmission rate was influenced by the area and diameter of the microholes. The 80PBS/20PBAT film, when perforated using laser fluence ranging from 184 J/cm² (resulting in a microhole area of 19,375 ± 804 μm²) to 370 J/cm² (resulting in a microhole area of 46,421 ± 3854 μm²), exhibited an increase in oxygen transmission rate (OTR) and carbon dioxide transmission rate (CO₂TR). The OTR values for the perforated film, containing 1 microhole/103 cm², increased from 106 ± 13 to 271 ± 7, and the CO₂TR values increased from 284 ± 6 to 390 ± 33 cm³/103 cm²·d. With an increment of microholes in the test area of 103 cm², the gas transmission rate increased. For example, the oxygen and carbon dioxide transmission rate of 80PBS/20PBAT containing 5 microholes were approximately 1332 ± 199 and 1285 ± 127 cm³/d, respectively. The CO₂TR/OTR values of microperforated PLA

Table 4. Oxygen and Carbon Dioxide Transmission Rates of Microperforated 80PBS/20PBAT Film

Sample film	Number of microholes/package	Number of microholes/m ²	Oxygen transmission rate, OTR (cm ³ /m ² ·d)	Carbon dioxide transmission rate, CO ₂ TR (cm ³ /m ² ·d)	CO ₂ TR/OTR, β
80PBS/20PBAT	0	0	5900	16,400	2.78
80PBS/20PBAT-MP1	20	300	68,900	82,500	1.20
80PBS/20PBAT-MP2	40	600	131,900	148,500	1.13

and PBS films decreased to 1, which is consistent with the trend observed in commercial microperforated films.³⁴

The gas transmission rate of a single microhole was assessed by calculating the difference between the transmission rate of the neat 80PBS/20PBAT film and that of the perforated film. When the film was perforated using a laser fluence of 184 J/cm², a single microhole exhibited OTR and CO₂TR values through only microhole of 45 ± 13 and 115 ± 15 cm³/d, respectively. With an increase in laser fluence to 370 J/cm², the microhole area expanded to $46,421 \pm 3854$ μ m², leading to high gas transmission rates of 210 ± 7 cm³/d for OTR and 220 ± 33 cm³/d for CO₂TR. The gas transmission rate findings correlated with the microhole area.³⁸

3.3. Packaging Applications. With regard to the equilibrium modified atmosphere packaging (EMAP) principle, suitable packaging films for many types of fresh produce should have high OTR in a range of $\sim 10,000$ cm³/m²·d at a thickness of ~ 25 μ m.³⁴ Therefore, different biodegradable films with varying numbers of microholes were developed to evaluate the effectiveness of microperforated 80PBS/20PBAT film as a packaging material to extend the shelf life of mangoes via equilibrium modified atmosphere packaging. In this experiment, mangoes weighing between 300 and 350 g were packed using microperforated 80PBS/20PBAT films identified as 80PBS/20PBAT, 80PBS/20PBAT-MP1, and 80PBS/20PBAT-MP2 for packaging size of 15 × 22 cm. Gas transmission rates of the tested films are shown in Table 4. The microperforated films had microhole densities corresponding to 20 and 40 microholes/package for 80PBS/20PBAT-MP1 and 80PBS/20PBAT-MP2, respectively. After packaging, the samples were stored at 13 °C, and the gas compositions inside the package (O₂ and CO₂) were monitored throughout the storage period. The weight loss percentage, freshness quality, and visual appearance of the mangoes were also assessed.

3.3.1. Gas Composition Inside the Packages. Several factors including gas permeability of the packaging film, mango weight, respiration rate, storage temperature, and headspace volume influenced the gas composition within the package.³⁹ Gas compositions in packages using nonperforated 80PBS/20PBAT film and two different microperforated 80PBS/20PBAT films are shown in Figure 5. During the 35 day storage period, gas composition in the packaging was monitored. The package initially contained 21% O₂ and 0.03% CO₂. By day 3 of storage, the O₂ content in the nonperforated package with low gas transmission rate (OTR of 5900 cm³/m²·d and CO₂TR of 16,400 cm³/m²·d) decreased to 0.3% while the CO₂ content increased to 32% because the produce consumed the available oxygen and produced carbon dioxide through respiration. Low O₂ levels and high CO₂ levels during storage accelerated mango deterioration. By day 4, the mango in the 80PBS/20PBAT film package exhibited an unsatisfactory freshness quality with detection of a fermentative odor, while the microperforated 80PBS/20PBAT film

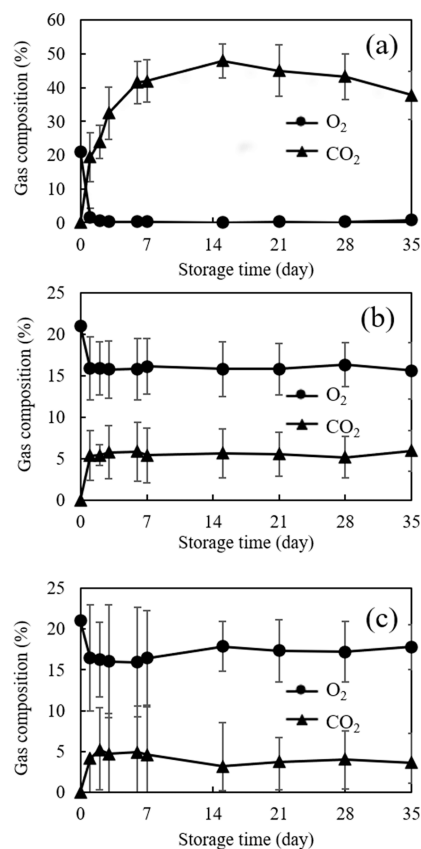


Figure 5. In-pack gas concentrations in (a) 80PBS/20PBAT, (b) 80PBS/20PBAT-MP1, and (c) 80PBS/20PBAT-MP2 packages at 13 °C for 35 days.

resulted in an equilibrium modified atmosphere in all packages. The O₂ concentration gradually decreased and stabilized at 15% in 80PBS/20PBAT-MP1 and 17% in 80PBS/20PBAT-MP2 packaging films throughout the 35-day storage period. By day two of storage, the CO₂ concentration increased and reached an equilibrium atmosphere, with levels of 6% in MP1 and 4% in MP2 packaging films. The microperforated films with a high gas transmission rate allowed gas exchanges through the films at rates that matched the rate of mango respiration. These findings indicated that microperforated film packages dissipated anaerobic or fermentative respiration, ensuring better preservation of mango quality.

3.3.2. Changes in the Quality of Packed Mango. Factors such as fruit maturity and ripening and storage conditions greatly influence fruit firmness.⁴⁰ The assessment of mango quality by consumers mainly considers firmness (Figure 6) as an important characteristic. Softening occurs quickly after harvest in mango due to biochemical changes such as the degradation of pectin, cellulose, and hemicellulose.^{41,42} From these results, the mango pulp packed in the 80PBS/20PBAT film was firmer than mango packed in the 80PBS/20PBAT-

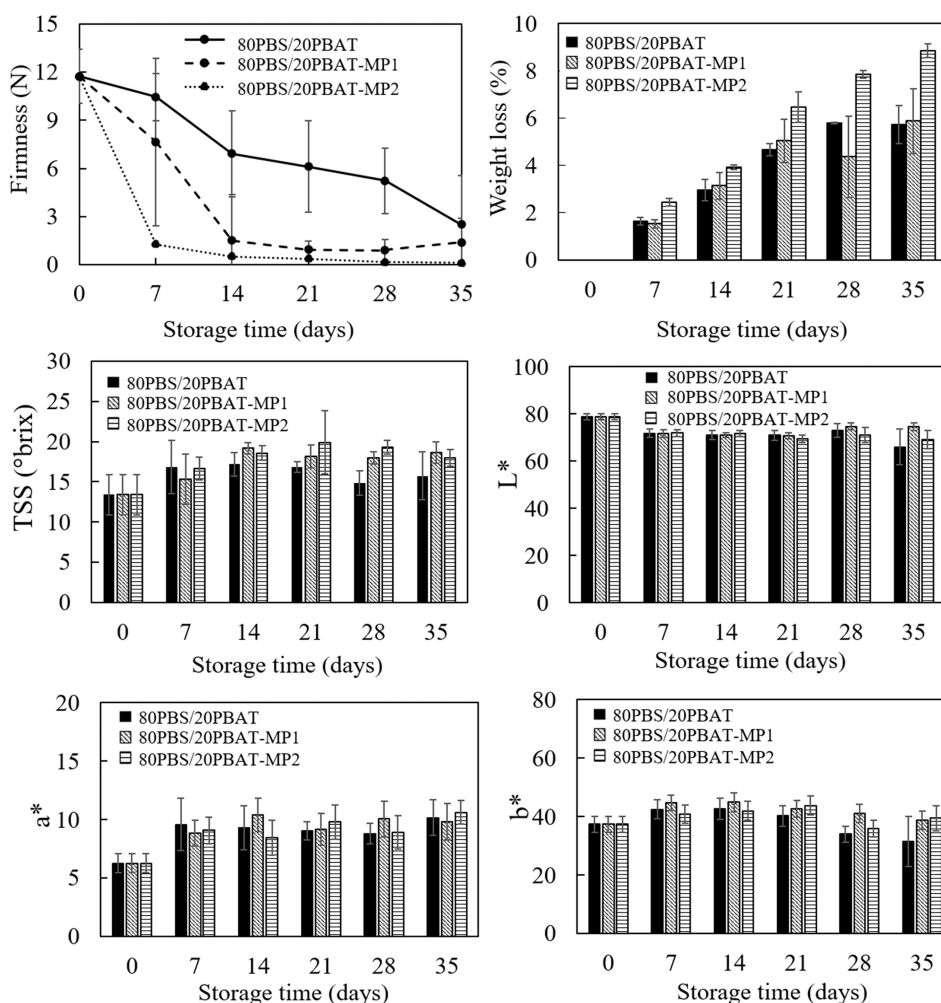


Figure 6. Freshness quality (color, TSS, firmness, and weight loss) of packed mango throughout the storage period.






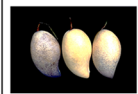












MP1 and 80PBS/20PBAT-MP2 packages, possibly due to the occurrence of fermented metabolism of the mango pulp within the package containing lower O_2 levels (0%) and high CO_2 levels (32%), resulting in off-flavor development after day 3 (as can be seen in Figure 5). In addition, the firmness of mango packed in 80PBS/20PBAT-MP1 was higher than that of mango packed in the 80PBS/20PBAT-MP2 package. The 80PBS/20PBAT-MP1 film with a lower gas transmission rate can reduce respiration rate and maintain firmness by reducing the escape of moisture and gases that contribute to softening and deterioration. Reduced oxygen and elevated carbon dioxide in the packages delayed the respiration rates of fruits, which resulted in delayed maturation and ripening of fruits.

Weight loss is a critical factor influencing mango storage shelf life and freshness quality, caused primarily by respiration and transpiration processes. During storage, weight loss increased under all treatments (Figure 6). Packages sealed with the 80PBS/20PBAT film exhibited the lowest weight loss compared to the 80PBS/20PBAT-MP1 and 80PBS/20PBAT-MP2 packages, attributed to the low water vapor transmission rate (WVTR) of the 80PBS/20PBAT film without microholes, allowing for minimal water loss from the package. However, the mango in the 80PBS/20PBAT film package had an unsatisfactory freshness quality with a detectable fermentative odor, whereas the microperforated 80PBS/20PBAT films maintained an equilibrium modified atmosphere in all

packages. The microperforated film 80PBS/20PBAT-MP2 packages, with a high gas transmission rate, experienced high 10% pulp weight loss during the 35-day experiment. Mangoes stored using 80PBS/20PBAT-MP1 showed the lowest weight loss of nearly 6% after 35 days of storage, which met the acceptable commercial requirement of less than 10%.

Changes in total soluble solids (TSS), sugars represent most of the total soluble solids in fruit juices, making it practical to estimate sweetness using the soluble solid content. The mango initially had a total soluble solid content of 14 $^{\circ}$ brix, which gradually increased to 20 $^{\circ}$ brix and remained constant during storage in microperforated films (Figure 6). There were no significant differences between the three packages. Moreover, mango pulp color changes were determined using L^* , a^* , and b^* values (Figure 6). The three package types did not exhibit any significant differences in the mango pulp color. Figure 6 depicts the distinction of lightness (L^*), redness (a^*), and yellowness (b^*) of the mango color. L^* , a^* , and b^* values were employed to describe the different color characteristics. The L^* value of the mango pulp continuously decreased during storage, indicating flesh browning. Carotenoid oxidation is primarily responsible for the loss of mango color, leading to a gradual decrease in value.⁴³ The a^* value exhibited a gradual increase. The positive a^* value indicated the presence of the red color in the samples, which implied the development of a

Table 5. Appearance of Mango Throughout the Storage Period

Film	Day 0	Day 7	Day 14	Day 21	Day 28	Day 35
80PBS/20PBAT						
80PBS/20PBAT-MP1						
80PBS/20PBAT-MP2						

brown color throughout the entire storage period, while the b^* value remained unchanged in all packages.

As for the visual appearance of the mango, no significant difference was found in mango skin color during the storage period, while mangoes packed in 80PBS/20PBAT without a microhole showed a reduction in freshness quality, mainly from the off-odor on day 3 of storage. Mangoes packed in 80PBS/20PBAT-MP2 showed decay primarily due to anthracnose and partial stem-end rot on day 28, as exhibited in Table 5. The mango individually packed in 80PBS/20PBAT-MP1 showed delayed freshness quality deterioration. Findings demonstrated that 80PBS/20PBAT-MP1 significantly increased the shelf life of mangoes up to 35 days. Prolonged shelf life allows exporters to benefit from cost-effective transportation using sea freight rather than air freight. The study results underscore the potential of packaging and distribution technologies in facilitating the supply of superior fresh fruits and vegetables to global markets.

4. CONCLUSIONS

The incorporation of PBAT into the PBS material led to significant improvements in its mechanical properties. The resulting film, composed of 80 wt % PBS and 20 wt % PBAT (80PBS/20PBAT), exhibited optimal mechanical characteristics. As for microperforated films, the study demonstrated that the 80PBS/20PBAT material had excellent energy absorption capacity for CO₂ lasers, with laser fluence adjustments leading to a substantial increase in microhole size. Utilizing laser perforation significantly improved the oxygen and carbon dioxide transmission rate (OTR and CO₂TR) in the 80PBS/20PBAT film, ultimately extending the shelf life of mangoes for up to 35 days. The study's findings hold promise for improving the preservation and quality of perishable goods like mangoes, contributing to more sustainable and efficient packaging solutions.

■ AUTHOR INFORMATION

Corresponding Author

Charinee Winotapun – National Metal and Materials Technology Center, National Science and Technology Development Agency, Pathum Thani 12120, Thailand; orcid.org/0000-0002-0626-5566; Email: Charinew@mtec.or.th

Authors

Methinee Tameesrisuk – National Metal and Materials Technology Center, National Science and Technology Development Agency, Pathum Thani 12120, Thailand

Pakjira Sirirutbunkajal – National Metal and Materials Technology Center, National Science and Technology Development Agency, Pathum Thani 12120, Thailand

Pichamon Sungdech – Department of Packaging and Materials Technology, Faculty of Agro-Industry, Kasetsart University, Bangkok 10900, Thailand

Pattarin Leelaphiwat – Department of Packaging and Materials Technology, Faculty of Agro-Industry, Kasetsart University, Bangkok 10900, Thailand; Center for Advanced Studies for Agriculture and Food, Kasetsart University, Bangkok 10900, Thailand

Complete contact information is available at:

<https://pubs.acs.org/10.1021/acsomega.3c06999>

Notes

The authors declare no competing financial interest.

■ ACKNOWLEDGMENTS

Funding for this study was provided by the National Research Council of Thailand (NRCT) (Grant No. N21A660714). All equipment was supported by the National Metal and Materials Technology Center (MTEC), National Science and Technology Development Agency (NSTDA), Thailand.

■ REFERENCES

- Belay, Z. A.; Caleb, O. J.; Opara, U. L. Modelling approaches for designing and evaluating the performance of modified atmosphere packaging (MAP) systems for fresh produce: A review. *Food Packaging and Shelf Life* **2016**, *10*, 1–15.
- Winotapun, C.; Aontee, A.; Inyai, J.; Pinsuwan, B.; Daud, W. Laser perforation of polyethylene terephthalate/polyethylene laminated film for fresh produce packaging application. *Food Packaging and Shelf Life* **2021**, *28*, 100677.
- Winotapun, C.; Issaraseree, Y.; Sirirutbunkajal, P.; Leelaphiwat, P. CO₂ laser perforated biodegradable films for modified atmosphere packaging of baby corn. *Journal of Food Engineering* **2023**, *341*, 111356.
- Mistriotis, A.; Briassoulis, D.; Giannoulis, A.; D'Aquino, S. Design of biodegradable bio-based equilibrium modified atmosphere packaging (EMAP) for fresh fruits and vegetables by using micro-perforated poly-lactic acid (PLA) films. *Postharvest Biology and Technology* **2016**, *111*, 380–389.
- Mahajan, P. V.; Oliveira, F. A. R.; Montanez, J. C.; Frias, J. Development of user-friendly software for design of modified

- atmosphere packaging for fresh and fresh-cut produce. *Innovative Food Science & Emerging Technologies* **2007**, *8* (1), 84–92.
- (6) Al-Ati, T.; Hotchkiss, J. H. The Role of Packaging Film Permeability in Modified Atmosphere Packaging. *J. Agric. Food Chem.* **2003**, *51* (14), 4133–4138.
- (7) Rodov, V.; Porat, R.; Sabag, A.; Kochanek, B.; Friedman, H. Microperforated Compostable Packaging Extends Shelf Life of Ethylene-Treated Banana Fruit. *Foods* **2022**, *11* (8), 1086.
- (8) Dhalsamant, K.; Mangaraj, S.; Bal, L. M. Modified Atmosphere Packaging for Mango and Tomato: An Appraisal to Improve Shelf Life. *J. Packaging Technol. Res.* **2017**, *1* (3), 127–133.
- (9) Pinto, L.; Palma, A.; Cefola, M.; Pace, B.; D'Aquino, S.; Carboni, C.; Baruzzi, F. Effect of modified atmosphere packaging (MAP) and gaseous ozone pre-packaging treatment on the physico-chemical, microbiological and sensory quality of small berry fruit. *Food Packaging and Shelf Life* **2020**, *26*, 100573.
- (10) Xing, Y.; Li, X.; Xu, Q.; Jiang, Y.; Yun, J.; Li, W. Effects of chitosan-based coating and modified atmosphere packaging (MAP) on browning and shelf life of fresh-cut lotus root (*Nelumbo nucifera* Gaerth). *Innovative Food Science & Emerging Technologies* **2010**, *11* (4), 684–689.
- (11) Baite, T. N.; Mandal, B.; Purkait, M. K. Antioxidant-Incorporated Poly(vinyl alcohol) Coating: Preparation, Characterization, and Influence on Ripening of Green Bananas. *ACS Omega* **2022**, *7* (46), 42320–42330.
- (12) Chinsirikul, W.; Klintham, P.; Kerddonfag, N.; Winotapun, C.; Hararak, B.; Kumsang, P.; Chonhenchob, V. Porous Ultrahigh Gas-Permeable Polypropylene Film and Application in Controlling In-pack Atmosphere for Asparagus. *Packaging Technology and Science* **2014**, *27* (4), 313–325.
- (13) Tian, B.; Liu, J.; Yang, W.; Wan, J.-B. Biopolymer Food Packaging Films Incorporated with Essential Oils. *J. Agric. Food Chem.* **2023**, *71* (3), 1325–1347.
- (14) Dmitruk, A.; Ludwiczak, J.; Skwarski, M.; Makula, P.; Kaczyński, P. Influence of PBS, PBAT and TPS content on tensile and processing properties of PLA-based polymeric blends at different temperatures. *J. Mater. Sci.* **2023**, *58* (4), 1991–2004.
- (15) Threepopnatkul, P.; Preedanorawut, R. Poly(lactic acid) and polybutylene succinate films incorporated with modified zeolite. *Materials Today: Proceedings* **2022**, *65*, 2309–2314.
- (16) Xiao, L.; Yao, Z.; He, Y.; Han, Z.; Zhang, X.; Li, C.; Xu, P.; Yang, W.; Ma, P. Antioxidant and antibacterial PBAT/lignin-ZnO nanocomposite films for active food packaging. *Industrial Crops and Products* **2022**, *187*, 115515.
- (17) Yang, F.; Chen, G.; Li, J.; Zhang, C.; Ma, Z.; Zhao, M.; Yang, Y.; Han, Y.; Huang, Z.; Weng, Y. Effects of Quercetin and Organically Modified Montmorillonite on the Properties of Poly(butylene adipate-co-terephthalate)/Thermoplastic Starch Active Packaging Films. *ACS Omega* **2023**, *8* (1), 663–672.
- (18) Bumbudsanpharoke, N.; Wongphan, P.; Promhuad, K.; Leelaphiwat, P.; Harnkarnsujarit, N. Morphology and permeability of bio-based poly(butylene adipate-co-terephthalate) (PBAT), poly(butylene succinate) (PBS) and linear low-density polyethylene (LLDPE) blend films control shelf-life of packaged bread. *Food Control* **2022**, *132*, 108541.
- (19) Messin, T.; Marais, S.; Follain, N.; Guinault, A.; Gaucher, V.; Delpoue, N.; Sollogoub, C. Biodegradable PLA/PBS multilayer membrane with enhanced barrier performances. *J. Membr. Sci.* **2020**, *598*, 117777.
- (20) Ozdemir, I.; Monnet, F.; Gouble, B. Simple determination of the O₂ and CO₂ permeances of microperforated pouches for modified atmosphere packaging of respiring foods. *Postharvest Biology and Technology* **2005**, *36* (2), 209–213.
- (21) González-Buesa, J.; Salvador, M. L. A multiphysics approach for modeling gas exchange in microperforated films for modified atmosphere packaging of respiring products. *Food Packaging and Shelf Life* **2022**, *31*, 100797.
- (22) Boonthanakorn, J.; Daud, W.; Aontee, A.; Wongs-Aree, C. Quality preservation of fresh-cut durian cv. 'Monthong' using micro-perforated PET/PE films. *Food Packaging and Shelf Life* **2020**, *23*, 100452.
- (23) Rivera, C. S.; Blanco, D.; Salvador, M. L.; Venturini, M. E. Shelf-Life Extension of Fresh Tuber *aestivum* and Tuber *melanosporum* Truffles by Modified Atmosphere Packaging with Micro-perforated Films. *J. Food Sci.* **2010**, *75* (4), No. E225-E233.
- (24) González, J.; Ferrer, A.; Oria, R.; Salvador, M. Determination of O₂ and CO₂ transmission rates through microperforated films for modified atmosphere packaging of fresh fruits and vegetables. *Journal of Food Engineering* **2008**, *86*, 194–201.
- (25) Winotapun, C.; Watcharasin, U.; Kerddonfag, N.; Chinsirikul, W.; Takarada, W.; Kikutani, T. Microhole formation behavior of polypropylene film using CO₂ laser irradiation. *Journal of Fiber Science and Technology* **2017**, *73* (10), 240–250.
- (26) Dang, K. T. H.; Singh, Z.; Swinny, E. E. Edible Coatings Influence Fruit Ripening, Quality, and Aroma Biosynthesis in Mango Fruit. *J. Agric. Food Chem.* **2008**, *56* (4), 1361–1370.
- (27) Datir, S.; Regan, S. Advances in Physiological, Transcriptomic, Proteomic, Metabolomic, and Molecular Genetic Approaches for Enhancing Mango Fruit Quality. *J. Agric. Food Chem.* **2023**, *71* (1), 20–34.
- (28) González-Aguilar, G. A.; Fortiz, J.; Cruz, R.; Baez, R.; Wang, C. Y. Methyl Jasmonate Reduces Chilling Injury and Maintains Postharvest Quality of Mango Fruit. *J. Agric. Food Chem.* **2000**, *48* (2), 515–519.
- (29) Suwapanich, R.; Haewsungcharoen, M. Effect of temperature and storage time on the thermal properties of Mango Nam Dok Mai cv. Si Thong during storage. *J. Agric. Technol.* **2007**, *3* (1), 137–142.
- (30) Boonruang, K.; Chonhenchob, V.; Singh, S. P.; Chinsirikul, W.; Fuongfuchat, A. Comparison of Various Packaging Films for Mango Export. *Packaging Technology and Science* **2012**, *25* (2), 107–118.
- (31) Phakdee, N.; Chairasart, P. Modified Atmosphere Storage Extends the Shelf Life of 'Nam Dok Mai Sri Tong' Mango Fruit. *Int. J. Fruit Science* **2019**, *20* (3), 495–505.
- (32) P, S.; Baskaran, R.; M, R.; Prashanth, K. H.; R, T. Storage studies of mango packed using biodegradable chitosan film. *European Food Research and Technology* **2002**, *215* (6), 504–508.
- (33) D'Aquino, S.; Mistriotis, A.; Briassoulis, D.; Di Lorenzo, M. L.; Malinconico, M.; Palma, A. Influence of modified atmosphere packaging on postharvest quality of cherry tomatoes held at 20°C. *Postharvest Biology and Technology* **2016**, *115*, 103–112.
- (34) Winotapun, C.; Kerddonfag, N.; Kumsang, P.; Hararak, B.; Chonhenchob, V.; Yamwong, T.; Chinsirikul, W. Microperforation of Three Common Plastic Films by Laser and Their Enhanced Oxygen Transmission for Fresh Produce Packaging. *Packaging Technology and Science* **2015**, *28* (4), 367–383.
- (35) Boonprasertpoh, A.; Pentrakoon, D.; Junkasem, J. Investigating rheological, morphological and mechanical properties of PBS/PBAT blends. *J. Metals, Materials and Minerals* **2017**, *27*, 1–11.
- (36) Boonprasertpoh, A.; Pentrakoon, D.; Junkasem, J. Effect of PBAT on physical, morphological, and mechanical properties of PBS/PBAT foam. *Cellular Polymers* **2020**, *39* (1), 31–41.
- (37) Winotapun, C.; Kerddonfag, N.; Daud, W.; Chinsirikul, W.; Takarada, W.; Kikutani, T. Effect of biaxial-simultaneous stretching conditions on OTR and CO₂ permeation of CO₂ laser perforated poly(lactic acid) film. *Packaging Technology and Science* **2018**, *31* (8), 545–556.
- (38) Ghosh, V.; Anantheswaran, R. Oxygen Transmission Rate through Micro-Perforated Films: Measurement and Model Comparison. *Journal of Food Process Engineering* **2001**, *24*, 113–133.
- (39) Perumal, A. B.; Nambiar, R. B.; Sellamuthu, P. S.; Emmanuel, R. S. Use of modified atmosphere packaging combined with essential oils for prolonging post-harvest shelf life of mango (cv. Banganapalli and cv. Totapuri). *LWT* **2021**, *148*, 111662.
- (40) Yohanes, H.; Chu, C.-Y.; Pranamuda, H.; Lai, M.-F.; Harianto; Handayani, W. Application of edible coating and active packaging to extend shelf life of mango under atmosphere temperature. *Int. J. Energy Environ. Commun.* **2021**, *2* (3), 1–5.

(41) Labaky, P.; Grosmaire, L.; Ricci, J.; Wisniewski, C.; Louka, N.; Dahdouh, L. Innovative non-destructive sorting technique for juicy stone fruits: textural properties of fresh mangos and purees. *Food and Bioprocess Processing* **2020**, *123*, 188–198.

(42) Penchaiya, P.; Tijssens, L. M. M.; Uthairatanakij, A.; Srilaong, V.; Tansakul, A.; Kanlayanarat, S. Modelling quality and maturity of 'Namdokmai Sithong' mango and their variation during storage. *Postharvest Biology and Technology* **2020**, *159*, 111000.

(43) Nupur, A. Effect of Potassium Meta-bisulphite on Quality and Acceptability of Formulated Green Mango Pulp During Freezing. *J. Bangladesh Agril. Univ.* **2020**, *18* (3), 734–741.